Morphology and defect structures of novel relaxor ferroelectric single crystals $Pb(Mg_{1/3}Nb_{2/3})O_3$-$PbTiO_3$ *

XU Guisheng (许桂生)[1,2], LUO Haosu (罗豪甦)[1], ZHONG Weizhuo (仲维卓)[1], YIN Zhiwen (殷之文)[1], XU Haiqing (徐海清)[1], QI Zhenyi (齐振一)[1] and LIU Ke (刘 克)[1]

(1. Laboratory of Functional Inorganic Materials, Shanghai Institute of Ceramics, Chinese Academy of Sciences, Shanghai 201800, China; 2. Xiangtan Polytechnic Institute, Xiangtan 411201, China)

Received April 7, 1999

Abstract High-performance relaxor ferroelectric single crystals $Pb(Mg_{1/3}Nb_{2/3})O_3$-$PbTiO_3$ have been grown successfully by a modified Bridgman method. They have the size of $25 \times 25 \times 50$ mm^3 and are of pure perovskite phases with tetragonal or rhombohedral structures. Their {001} faces appear dominantly, which can be interpreted by the model of anionic coordination polyhedral growth units. Main macro defects observed under optical microscopes and SEM can be reduced or removed by improving growth parameters after understanding their formation mechanism. 71° or 109° macrodomains in rhombohedral PMNT 76/24 crystals and 90° macrodomains in tetragonal PMNT 65/35 crystals have been observed by optical microscopes. It has been found that the transition from microdomains to macrodomains can be induced by compositions. Both the imaging mechanism of non-180° domains and the relation between domain configurations and ferroelectric phase transition have been analyzed.

Keywords: relaxor ferroelectrics, single crystals, PMNT, morphology, defect structures, domain configurations.

Novel relaxor ferroelectric single crystals $(1-x)Pb(Mg_{1/3}Nb_{2/3})O_3$-$xPbTiO_3$, $(1-y)Pb(Zn_{1/3}Nb_{2/3})O_3$-$yPbTiO_3$ have been grown successfully, which has been regarded as an exciting great breakthrough in the 50-year history of the ferroelectric field[1]. They exhibit excellent piezoelectric properties, far better than those available from conventional piezoelectric ceramics (d_{33} from 700 pC/N up to 1 500 pC/N, k_{33} from 0.70 up to 0.92), and may lead to a revolution in ultrasonic transducers and related materials. If these crystals are used as probe materials instead of PZT ceramics, medical ultrasonic imaging transducers will have higher sensitivity and larger bandwidth[2], as will sonars and nondestructive defect inspections.

PMNT crystals with the complex perovskite structure, are cubic phases (m3m) above their Curie point (T_C) and rhombohedral (3 m) or tetragonal (4 mm) phases below T_C, depending on the value of x. There is a morphotropic phase boundary (MPB) around $x = 0.35$, where they exhibit optimum piezoelectric properties. For material fabrication, PMN-PT solid solution has many unfavorable factors, such as multi-components or complex compositions, incongruent melting, segregation and volatility. As a result, a harmful phase-pyrochlore is hard to avoid in the preparation of PMNT ceramics and it is very difficult to grow their single crystals with pure perovskite structures. As for the growth of relaxor single crystals, PZNT has been closely examined whereas PMNT has been

* Project supported by the National Natural Science Foundation of China (No.59995520), the Chinese Academy of Sciences and Shanghai Municipal Government.

considered rarely. Of present growth methods, high-temperature solution or flux methods are predominant, kyropoulos are secondary. Hydrothermal and HIP methods have also been used to prepare their crystallite powders. Up to now these methods have not been perfectly used. For example, the single crystals grown by the flux methods reached the size of 20—40 mm, but the spontaneous nucleation has not been controlled effectively, and the size and color vary in company with a little pyrochlore, the properties were unstable and the growth rate lower[3,4]. Recently there was a report about Bridgman method to grow PZNT crystals[5]. However some problems, which may arise from adding too much flux PbO to their starting materials, still left unresolved the problem of maintaining large size and composition homogeneity. It has been deduced that PMNT crystals are comparable with PZNT crystals in the properties of piezoelectric and electromechanical coupling and are more readily grown and are more suitable for Bridgman methods due to the characterization of PMNT in crystallochemistry. Based on these accounts, we took the lead in using a Bridgman method to grow PMNT crystals. The PMNT single crystals grown by this method were large in size and excellent in properties: the piezoelectric constant $d_{33} > 2\ 000$ pC/N, dielectric constant $\varepsilon = 5\ 300$, dielectric loss $\tan\delta < 0.8\%$, electromechanical factor $k_t = 0.64$, $k_{33} = 0.93$. This paper will report their characterizations in crystallography including their morphology, growth habits and structural defects related to their properties.

1 crystal growth and experimental

A modified Bridgman technique was used to grow PMNT crystals. The compositions were chosen near their MPB (76/24—65/35) to obtain optimum piezoelectric properties. Starting materials, including pure powders of PbO, MgO, Nb_2O_5 and TiO_2, were synthesized to PMNT powders under about 1 200℃ and then put in cylindrical platinum crucibles. The temperature in the upper part of the descending furnaces was higher than the melting point 1 290℃. The descending rate of Pt crucibles was engineered to make the shape of solid-liquid interfaces be slightly convex and their positions kept stable where the temperature gradient was the largest on the temperature curves of the furnaces. Some measures have been adopted to suppress the volatilization of PbO and the leak of crucibles, which are often encountered due to the erosion of crucibles by PbO.

The morphology of as-grown PMNT crystals was observed under scanning electron microscopes (SEM), their structure measured by XRD, the thermal stability analyzed by thermal gravity (TG) and differential thermal analysis (DTA). Such orientations as {001} or {111} were determined by X-ray orientation devices combined with XRD. The crystals were processed along these directions to polished plates with various thickness, standard plates (0.03 mm in thickness) or cube samples with six polished faces and edges 5—15 mm in length. The structural defects in these samples were then detected by cubic microscopes, polarizing microscopes, SEM or electron probe microanalysers (EPM).

2 Results and discussions

2.1 Morphology of crystals

The as-grown PMNT single crystals, being yellowish and transparent, had the density of 8.2 g/cm^3 and the size of 25 mm × 25 mm × 50 mm (fig. 1). This size was determined through X-ray orientation on different cuts of the same sample and observations on optical characterizations, crystal boundaries and domain configurations under polarizing microscopes.

The surface morphology atop the PMNT boules grown by the modified Bridgman technique showed that {001} faces appeared dominant and could constitute the surface morphology of positive and negative crystals (fig. 2). This morphology was formed by the freedom cooling of the remanent melts at the end of crucibles when the vertical temperature gradient in furnaces decreased greatly after the electricity was purposely cut off. If the whole melts froze normally, controlled by the fixed shift of the solid-liquid interfaces, the {001} faces would not appear at the end. In fact, the cut faces normal to the growth direction of boules grown without seeds were mainly {111}. In Bridgman techniques, crystals grew in the mechanism of geometric washout, thus, the crystals growing faster along the vertical temperature gradient would readily become larger. Therefore, PMNT crystals grow faster along [111] direction.

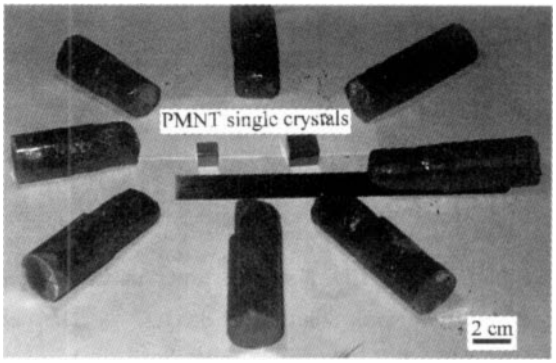

Fig. 1. As-grown PMNT crystal boules grown by a modified Bridgman technique.

The morphology and growth habits of PMNT crystals can be interpreted by the model of anionic coordination polyhedral growth units. The model considers that the morphology of crystals depends on the orientation of structure units in the crystals and that the growth units in the melts have the same structure units as the crystals themselves[6]. The structure of PMNT can be regarded as the one made of $[BO_6]$ coordination polyhedra linked by their vertexes (fig. 3). It has been found that the XRD spectrum on the powders of quenched PMNT samples directly from their melts is very similar to the one of PMNT crystals illustrated by fig.4, which means that there are growth units whose structural

Fig. 2. The surface morphology atop PMNT crystal boules observed under SEM.

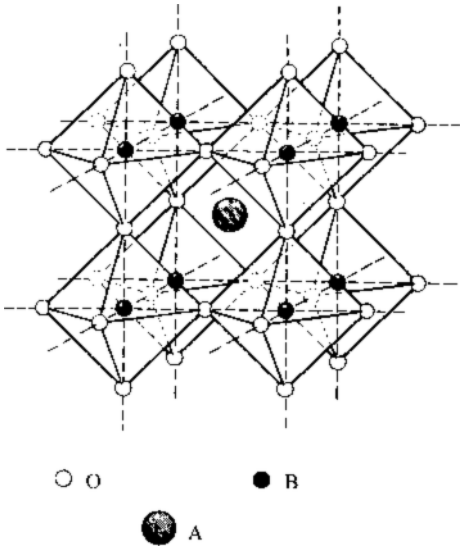

Fig. 3. The orientation and linking of $[BO_6]$ growth units in PMNT crystals.

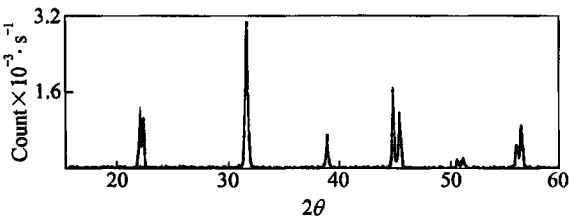

Fig. 4. The XRD spectrum of PMNT 65/35 crystals.

units are $[BO_6]$, in the growth melts. In fact, the surface structures atop the boules (fig. 2), which consist of series of triangle pyramids or the vertexes of cubes, are the locus of the combination of anionic coordination polyhedra $[BO_6]$ on the $\{111\}$ faces. As for $BaTiO_3$ with the same structures as PMNT, it has been stated indirectly that there were $[TiO_6]$ growth units in the growth solution by the experiments of applying electric fields on the growth solution of $BaTiO_3$[7]. The calculation on the stability energy of growth units also showed that $[TiO_6]$ could exist in the $BaTiO_3$ solution[8]. Based on the above data, it is very possible that there are $[BO_6]$ growth units, i.e. $[MgO_6]$, $[NbO_6]$ and $[TiO_6]$ octahedra, in PMNT melts.

This model considers that the rate of transport of growth units and their combination stability with growth interfaces depend on the growth rate of crystal faces and on the morphology. When $[BO_6]$ octahedra are combined with $\{111\}$, $\{110\}$ and $\{001\}$ faces, they link with the octahedra on the interfaces at 3, 2, and 1 free vertexes respectively. Thus, the stability energies of combination will decrease successively in this order so that the growth rates along these faces fall off in turn. As a result, once crystals gain the opportunity to grow freely, the $\{001\}$ face will appear dominant because it has the slowest growth rate. It should be pointed out that the result from above model is coincident with that from PBC theory. According to PBC theory, $\{111\}$, $\{110\}$ and $\{001\}$ faces in PMNT single crystals with simple cubic structure are kinked (K), stepped (S) and flat faces (F) respectively, their growth rates decreasing successively. It should be noticed that when $[BO_6]$ growth units cannot be built up for lack of Pb^{2+} arising from the high volatility of PbO, the negative surface morphology will appear atop the end of boules.

2.2 crystal structure and thermal stability

The XRD for the powders of as-grown PMNT single crystals showed that they were tetragonal phases (fig. 4) or rhombohedral ones depending on their compositions. They were pure perovskite structures, free of pyrochlore, on the level of XRD. It manifested that as for the effectiveness in suppressing the harmful pyrochlore, the Bridgman technique was equal to or better than the columbite precursor routes used in PMNT ceramics[9] and even better than the flux technique utilized to grow PZNT single crystals. The purpose of columbite precursor routes was to make oxides of B-sites react sufficiently, which was achieved through the melting of starting materials in the Bridgman technique. The better results of Bridgman technique for PMNT crystals also suggested that the thermal stability of PMNT crystals is higher than that of PZN or PZNT crystals. In the flux method used to grow PZNT crystals, the pyrochlore, which mixed with PbO and perovskite and could be extracted by hot nitric acid, was as much as 5% (in weight) at least[3]. It was also known that PZN started decomposing from 450℃ and generating pyrochlore and PbO, and that its obvious weight loss took place around 900℃[10]. However, the TG and DTA curves of PMNT crystals showed that their obvious weight loss came forth at around 1 200℃ and the TG curve hardly changed until this temperature (figure 5).

In our view, the distinction between PZNT and PMNT crystals in growth difficulties and thermal stability can be ascribed to the difference in their crystallochemistry, which can be reflected by the stability of their anionic coordination polyhedra. Of four kinds of octahedra, i.e. $[ZnO_6]$, $[MgO_6]$,

$[NbO_6]$ and $[TiO_6]$, the $[ZnO_6]$ octahedra are the most unstable since Zn^{2+} is apt to 4 coordination as is the case in pyrochlore. Therefore, in the PbO flux growth method, PZNT crystals are grown at metastable state, instead of stable state. Another advantage of PMNT over PZNT crystals is that their $PbTiO_3$ content exceeds that of PZNT crystals containing about 8 mol% $PbTiO_3$, because $PbTiO_3$ is favorable to the stability of these crystals. Adding the stable $[TiO_6]$ octahedral growth units to starting materials can adjust the linking between growth units $[MgO_6]$ and $[NbO_6]$, or $[ZnO_6]$ and $[NbO_6]$, which are unmatched in electric charge.

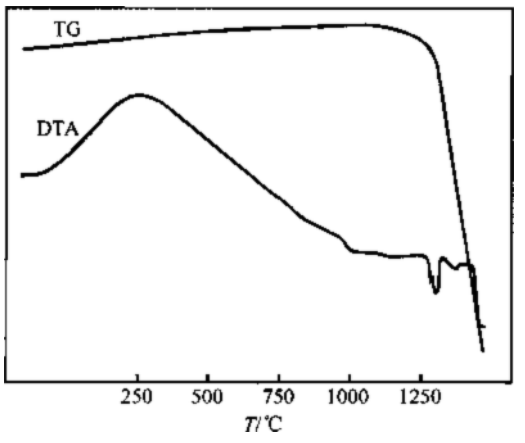

Fig. 5. Curves of TG and DTA of PMNT 67/33 crystals.

2.3 Inclusions in crystals

PMNT crystals grown by the aforementioned method contained a few inclusions, which could be subdivided into two types. The first one is solid inclusions. Tiny scattering particles smaller than 0.01 mm could be observed under the reflected light of polarizing microscopes and were distributed in a diffuse state. Light-bands around these particles could be visualized under crossed polarizing microscopes (fig. 6). The focus of stress near defects would change the optical characterization of crystals and generate these light-bands. The second one was gas inclusions. They were 1—3 μm in size visualized under SEM (fig. 7). These pores either took the shape of circles, or had angled edges formed in the process of grinding and polishing since the crystals were softer. The EDS results of EPM also testified that the compositions at pores were the same as crystals. No pyrochlore has yet been found in EDS.

Fig. 6. The scattering particles in PMNT crystals observed under crossed polarizing microscopes.

The intervals of melting points between different starting oxides are so large as to close near 2 000℃, from 886℃ of PbO to 2 830℃ of MgO. Thus, it is difficult for these oxides to melt entirely under the temperature slightly higher than the melting point of about 1 290℃ of PMNT crystals, which results in the formation of those tiny scattering particles. After the size of starting powders is decreased, the growth temperature enhanced or soaking time prolonged, the starting materials will tend to melt completely and the scattering particles will drop down.

The reasons for the formation of pores in PMNT crystals may be complicated. The air may come from the space among the powders of starting materials or the space of the unfilled parts of crucibles. On the other hand, oxygen can also be afforded by the decomposition of some oxides or PMNT crystals at the temperature higher than 1 200℃. By means of enhancing growth temperature or slowing down

Fig. 7. The pores in PMNT crystals under SEM.

growth rate, the bubbles will shift faster in the melts or diffuse more sufficiently so that the bubbles combined with crystals become fewer. However, it should be noted that too high a growth temperature might cause the decomposition of crystals and the formation of new bubbles.

2.4 Negative crystal structures

Some inclusions in PMNT crystals had regular faces and could be called negative crystal structures whose crystallographic orientation was coincident with that of the crystals themselves. The structures had two kinds of size, the big one being about 1.0 mm and the small one about 0.02 mm, and they were all red and PbO in compositions. The big negative structures could be visualized by naked eye, distributed solitarily and on {111} cuts appearing in the form of a triangle whose three sides were slightly convex. Sometimes, the negative crystals were hollow at their centers and developed growth striations near their sides (fig.8 (a)). After etching by hydrochloric acid, the color of these negative crystals became lighter and even disappeared. At last the etched structures changed into negative cavities whose sides were translated outwards when further etched. However, the small negative structures occurred frequently in strips (figure 8(b)).

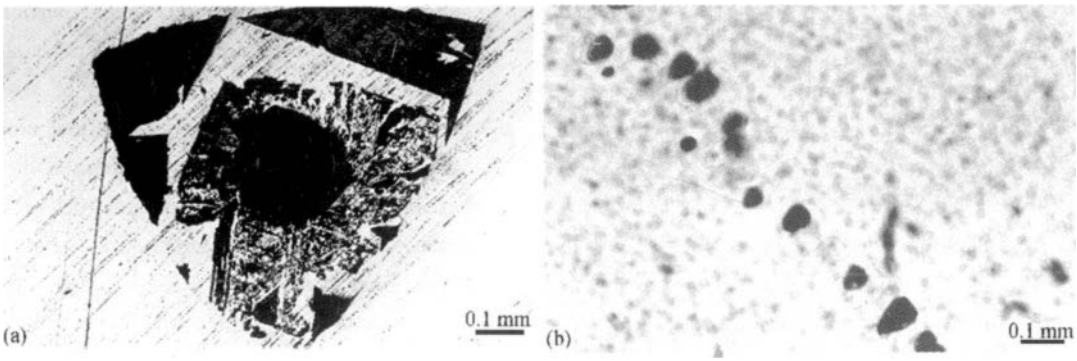

Fig. 8. The negative crystal structures (a) and their distribution (b) in PMNT crystals.

When the fluctuation in temperature during the growth process leads to the rapid supercooling of melts, some of melts having no time to crystallize may be surrounded by crystals in liquid state. In the subsequent cooling stage, these melts can freeze gradually at the inner crystals and form negative crystals. The small negative crystals in stripped arrangement are formed when the melts (mainly PbO) are encircled simultaneously at different places of growth interfaces. On understanding the relation between negative crystal structures and growth process or factors, one can decrease or eliminate them by adjusting or optimizing growth parameters to reduce the temperature fluctuation.

2.5 Ferroelectric domains

2.5.1 Observation on domains. In the cooling process from high temperature to the one lower than

Curie points, the transition from paraelectric phase to ferroelectric phase will take place in PMNT single crystals and form ferroelectric domains. The formation of 180° domain is to reduce the static electric energy enhanced by the ferroelectric phase transition, whereas the formation of non-180° domains (90° domains in tetragonal phases, 71° or 109° domains in rhombohedral ones) is to depress the increase of elastic energy caused by the same reason. The domain structures are important defects because they influence the poling, aging and other application properties of the crystals.

The non-180° domains can be observed by means of polarizing microscopes. It is found, when observed by naked eye, that the 90° macrodomains in tetragonal PMNT 65/35 crystals are less clear than those in $BaTiO_3$ crystals grown by TSSG methods. The former cannot be visualized until the samples are finely ground whereas the latter can be clearly shown on samples before being finely ground. However, the 90° domains in tetragonal PMNT 65/35 are more easily observed than the 71° or 109° domains in rhombohedral PMNT 76/24, which cannot be visualized under cubic microscopes or by naked eye.

Under crossed polarizing microscopes, the domains in the rhombohedral PMNT crystals can be shown and the domains in tetragonal crystals show more clearly. 90° domains (fig. 9 (a)), 71° or 109° domains (fig. 9 (b)) show as bright and black strips arranged alternatively. The radii of refraction ellipsoids in different domain strips are not parallel with each other, thus, the extinction positions in these strips are different. In addition, the observation on cubic samples with six {001} faces shows that the domain walls in the aforementioned PMNT single crystals, whether rhombohedral or tetragonal phases, are parallel with {110}.

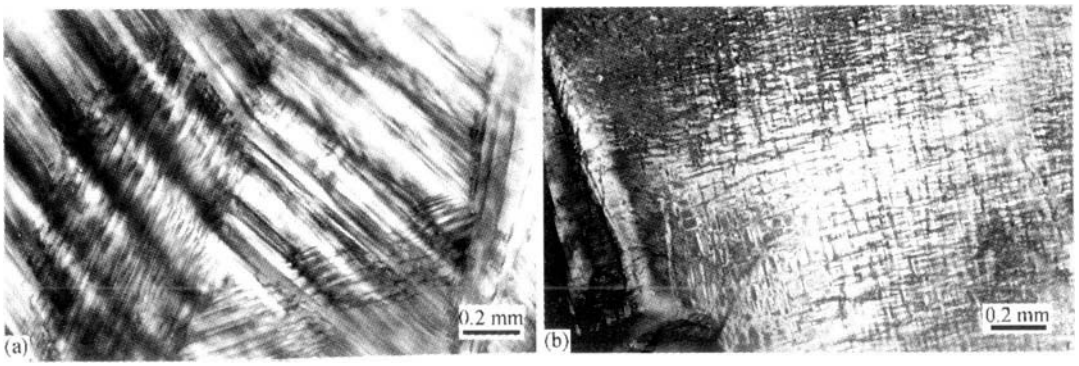

Fig. 9. The 90° domain configurations in PMNT 65/35 crystals (a) and 71° or 109° domain configurations in PMNT 76/24 crystals (b) under polarizing microscopes.

As for the observation on the domain configurations in PMNT 76/24 single crystals under crossed polarizing microscopes, the observing effect is related to plate thickness. When the plate thickness exceeds 1.0 mm, the domains are hardly shown and the samples present bright interference colors. If the polished plate is thinned to about 0.50 mm, the domains can be shown in the form of different interference strips. If the plate is further thinned down to the thickness of the standard plate (0.03 mm), the domain strips will take on wavy and irregular patterns with the width of about 0.01 mm (fig. 9 (b)). When the polished plate is thicker, several domains will overlap in the vertical direction, causing the interference colors to interfere with each other and making the domains show only with difficulty. The thinner the polished plate the clearer the domain configurations.

2.5.2 *Mechanism of the formation and imaging of domains.* It is known that under temperatures far lower than their Curie point T_C, PMN was still in optical isotropy since the symmetry of PMN only changed a little and was cubic in macro at the temperature near T_C even though its dielectric constant presented a peak near T_C. It is also known that only microdomains existed in pure PMN[11—13]. In our view, the optical anisotropy in rhombohedral PMNT crystals, revealed by the domains and interference colors, originates from the diffusion degree of ferroelectric phase transition in this crystal being lower than that of pure PMN crystals. After adding $PbTiO_3$ to PMN, $[MgO_6]$ and $[NbO_6]$ octahedra will be diluted by $[TiO_6]$ octahedra and become difficult to segregate or form an ordered arrangement. As a result, the composition fluctuation in the micro-range will be reduced and the effect of space or random field weakened, making the ferroelectric phase transition take place spontaneously. It is clear that in the rhombohedral range from pure PMN to PMNT 76/24, the transition from microdomains to macrodomains has taken place. The ferroelectric phase transition in pure PMN does not take place spontaneously, whereas, this transition in PMNT 76/24 does. In this context, we consider that the ferroelectric phase transition in PMNT crystals can be induced by adding $PbTiO_3$.

The domains in the rhombohedral phase PMNT are different from those in the tetragonal phase PMNT in the observation difficulties, and this phenomenon is related to the characterizations in crystal structures and ferroelectric phase transition. In crystal structures, the lattice constants a and c in tetragonal PMNT crystals show perceivable differences, which can be seen in the splitting of peaks in their XRD spectrum, but in rhombohedral PMNT, the lattice constants are $a = b = c$ and α is slightly deviated from 90°. Therefore, the anisotropy in tetragonal PMNT is larger than that in rhombohedral phases, and so is the largest birefraction index. A sharp change in the refraction indexes can take place on the 90° domain walls of tetragonal PMNT and cause the light to be entirely reflected and the 90° domain shown under reflected light. On the other hand, in rhombohedral phases (PMNT76/24), the light will not be reflected entirely by the domain walls, where there is a small change in refraction indexes, thus the domains can not show under reflected light. Only under transmission light are the domains in PMNT 76/24 shown. When the $PbTiO_3$ content in rhombohedral phases is near MPB, their domains can show unclearly under reflected light, a manifestation that the deviating degree of α from 90° and the largest birefraction index increase with $PbTiO_3$ content. From the point of the characterization of ferroelectric phase transition, the rhombohedral PMNT crystals are formed through diffuse phase transition from high temperature paraelectric phases, however, the tetragonal PMNT crystals are formed through normal ferroelectric phase transition. There are numerous polar microregions, which arrange along eight [111] directions arbitrarily and are heterogeneous in composition, in the inner of rhombohedral PMNT. The crystals may also contain some nonpolar regions too tiny to resolve. Therefore, as compared with tetragonal phases, the symmetry of the rhombohedral phases is closer to cubic prototype symmetry and their optical anisotropy is lower. By this token, the largest birefraction index in PMNT crystals reflects in certain degree the characterization of crystal structures and ferroelectric phase transition.

It can be observed that domain walls develop differently along symmetrical directions, frequently being denser along some directions but sparser along other directions. Besides that, the domains in single crystals PMNT tend to distribute heterogeneously, being mix of various domains, simple or complicated in configurations. Thus it can be seen that the formation of domains is affected not only

by the crystal symmetry, but also by such factors as practical temperature field (or anisotropy in temperature) and structural defects. While cooling through the Curie point, the spontaneous polarization in the crystals may prefer to switch to the direction of the largest temperature gradient and the related domain walls may be denser in distribution. Around the structural defects as inclusions or negative crystal structures, non-180° domain walls will be denser and even exist in the form of several groups of orientation states.

3 Conclusions

This paper has discussed the morphology and structure defects of PMNT single crystals and the conclusions are as follows. (i) The PMNT single crystals grown by the modified Bridgman technique have reached the size of 25 mm × 25 mm × 50 mm. These high-performance piezoelectric single crystals are transparent, pure perovskite, free of pyrochlore and with few crystal defects. They have rhombohedral or tetragonal structures. The successful growth of PMNT crystals can be attributed to their characterization in crystallochemistry, especially the stability of anionic coordination polyhedra. (ii) The morphology of PMNT single crystals shows that their {001} faces appear dominantly. The growth mechanism and habit can be interpreted by the model of anionic coordination polyhedral growth units. (iii) On understanding the mechanism of scattering particles, gas inclusions and negative crystal structures, one can reduce or eliminate them by adjusting growth parameters. (iv) Induced by adding $PbTiO_3$ to pure PMN, the ferroelectric phase transition can take place spontaneously and the domains change from microdomains to macrodomains. (v) As for rhombohedral and tetragonal PMNT crystals, they are different in crystal structures and type of ferroelectric phase transition, leading to the differences in the largest birefraction index and in the showing of their domain configurations under optical microscopes. Their non-180° domains can be observed clearly under crossed polarizing microscopes.

References

1 Service, R. E., Shape-changing crystals get shiftier, *Science*, 1997, March 28, 275: 1878.

2 Park, S.-E., Shrout, T. R., Characteristics of relaxor-based piezoelectric single crystals for ultrasonic transducers, *IEEE Transactions on Ultrasonics, Ferroelectrics, and Frequency Control*, 1997, 44(5): 1140.

3 Mulvihill, M. L., Park, S. E., Risch, G. et al., The role of processing variables in the flux growth of lead zinc niobate-lead titanate relaxor ferroelectric single crystals, *Jpn. J. Appl. Phys.*, 1996, 35(7): 3981.

4 Kobayashi, T., Shimanuki, S., Saitoh, S. et al., Improved growth of large lead zinc titanate piezoelectric single crystals for medical ultrasonic transducers, *Jpn. J. Appl. Phys.*, 1997, 36(9B): 6035.

5 Shimanuki, S., Saito, S., Yamashita, Y., Single crystal of the $Pb(Zn_{1/3}Nb_{2/3})O3$-$PbTiO_3$ system grown by the vertical Bridgman method and its characterization, *Jpn. J. Appl. Phys.*, 1998, 37(6A): 3382.

6 Zhong, W. Z., Liu, G. Z., Shi, E. W. et al., Growth units and formation mechanisms of the crystals under hydrothermal condition, *Science in China*, Ser. B, 1994, 37(11): 1288.

7 Zhong, W. Z., Xia, C. T., Shi, E. W. et al., Formation mechanism of barium titanate nanocrystals under hydrothermal conditions, *Science in China* (in Chinese), Ser. E, 1997, 27(1): 9.

8 Shi, E. W., Yuan, R. L., Xia, C. T. et al., Studies on the model of growth units of $BaTiO_3$ crystallites under hydrothermal conditions, *J. Phys.* (in Chinese), 1997, 46(1): 1.

9 Swartz, S. L., Shrout, T. R., Fabrication of perovskite lead magnium niobate, *Mat. Res. Bull.*, 1982, 17: 1245.

10 Jang, H. M., Oh, S. H., Moon, J. H., Thermodynamic stability and mechanisms of formation and decomposition of perovskite $Pb(Zn_{1/3}Nb_{2/3})O_3$ prepared by the PbO flux method, *J. Am. Ceram. Soc.*, 1992, 75: 82.

11 Ye, Z.-G., Relaxor ferroelectric $Pb(Mg_{1/3}Nb_{2/3})O_3$: properties and recent understanding, *Ferroelectrics*, 1996, 184: 193.

12 Cross, L. E., Relaxor ferroelectrics, *Ferroelectrics*, 1987, 76: 241.

13 Husson, E., Chubb, M., Morell, A., Superstructure in $PbMg_{1/3}Nb_{2/3}O_3$ ceramics revealed by high resolution electron microscopy, *Mat. Res. Bull.*, 1988, 23: 357.